Light Hazard Measurement on an Ophthalmic Instrument

David Melo[1], Pedro Vieira[2] and Filipe Soares[1]

[1]*Fraunhofer Portugal AICOS, Rua Alfredo Allen, 455/461, 4200-135, Porto, Portugal*
[2]*Department of Physics, Faculdade de Ciências e Tecnologia, Universidade Nova de Lisboa,*
Quinta da Torre, 2829-516, Caparica, Portugal

Keywords: Light Hazard Measurement, Ophthalmic Instruments, Fundus Camera.

Abstract: When the acquisition of images is performed on human body structures, the safety of the person on which the images are being obtained acquires fundamental importance. This condition gathers even more relevance when the goal of the image acquisition is related with health examination. To ensure that every physician, when imaging human structures is undoubtedly secure that it will not harm or cause any non-tolerable discomfort to the subject undergoing the exam, medical devices have to surpass a set of specific norms depending on the nature of the structure being examined. More specifically related with instruments for eye related diseases diagnostic and treatment, the ISO-15004-2 norm is the currently accepted. As some types of eye exams rely on highly concentrated radiation, its power has to be limited in order to prevent irreversible damage. In this paper, a Light Hazard Measurement for a specific prototype will be addressed, on which the power calculation method for the emitted radiation will be described and the compliance of the limiting norms will be verified. The main conclusion from the work here described is that the prototype can be classified as a Group 1 Ophthalmic Device according to the ISO-15004-2 norm.

1 INTRODUCTION

In the work presented in this paper, a fundus camera prototype named EyeFundusScope, currently under investigation by Fraunhofer Portugal AICOS, is submitted to a light hazard measurement. The goal of this procedure is to understand if the prototype can be used in screening and diagnostics situations, without provoking any harm to the agents participating on them, from patients to examiners.

The prototype uses light sources emitting at different wavelengths, with one of them emitting on a narrow region of the near infrared the electromagnetic spectrum and the other emitting broadband white light. The light sources used were Light Emission Diodes (LEDs) and the measurement of its power was performed with a photodiode power sensor. The emission spectrum of each light source was obtained using a spectrometer.

In this section the crucial principles and tools needed for the measurements are introduced and in the next ones, the procedure, the consequent results and the conclusions that may be obtained from them are described.

1.1 Eye Examination

The eyes along with the brain, the nervous system and its information transfer channels ensure one of the five ways human beings can acquire and understand information advent from its surrounding environment. Taking this into consideration, a regular eye examination is of unaccountable importance.

According to the American Academy of Ophthalmology every adult should perform an ocular evaluation, at least, every 5 years (Feder et al., 2016). The frequency of the examinations for patients with, one or more risk factors, such as diabetes or with an already diagnosed ophthalmological pathology should naturally be increased (Feder et al., 2016).

During screening actions and regular medical appointments, several regions of the eye are observed. Depending on the type of exam and the eye region the physician wants to observe, radiation may have to be directed towards the eye. For instance considering retinal examination, taking into account fundus low reflectance, the retina can only be observed when a considerable amount of light passes the pupil, enters the ocular globe and reaches the fundus of the eye (DeHoog and Schwiegerling, 2009; Hammer and Schweitzer, 2002; Preece and Claridge, 2002). For

the observation of more anterior structures the use of light is not so imperative for illumination but can also be used to understand several physiological mechanisms as occurs in pupillometry, on which the pupillary response to light of specific wavelengths is studied (Kelbsch et al., 2016; Rukmini et al., 2015).

1.2 Light Emission Diodes(LED)

Nowadays, Light Emission Diodes are available in a wide-range of wavelengths, existing an almost continuum spectrum of wavelength availability from near ultraviolet to near infrared existing also monochromatic emitters at deeper infrared wavelengths (Capitán-Vallvey and Palma, 2011).

They present several advantages when compared with the traditional incandescent lamps namely, a longer lifetime, higher brightness, lower power consumption and the possibility of electrical modulation at higher rates (Malinen et al., 1998; Patrick and Fardo, 2000). Its usage in Healthcare Applications is widespread not only as part of diagnosis instruments, but also for disease treatment, more importantly within the scopes of dermatology, ophthalmology and recently, neurology (Rahman et al., 2013; Saltmarche et al., 2017; Eells et al., 2004). The technique is named photobiomodulation and can be defined as the irradiation of tissue with low-intensity light in the infrared band, provoking alterations on the cellular functions (Desmet et al., 2006).

LED principle of operation is based on electroluminescence, the production of light by flow of electrons (Schubert, 2018). More specifically for the production of white light, a phosphor is usually added to a blue light LED chip. The phosphor is excited by the blue light coming from the chip and absorbs part of it. Due to the excitation, it emits light of other visible wavelengths, usually in the green and red regions of the electromagnetic spectrum that together with the blue light partially transmitted, generates white light (Chen, 2005; Schubert, 2018).

1.3 Photodiode Power Sensors

Photodiode Power Sensors are constituted by a semiconductor that produces a flow of electrons (current) dependent on the amount and wavelength of photons (light intensity) that reach its working surface (Senior, 1986). From the current produced the power can be obtained.

The power output of the photodiode power sensor reveals a high dependence on the wavelength of the radiation being measured. So, they can only be used, as a direct power meter, when the light source being

measured has a narrow emission band. With this in consideration, the photodiode operator can select the expected wavelength of the radiation (hereinafter described as λ_0). Although, as the suppliers normally provide information on the Sensor Spectral Response (Figure 1) methods for the measurement of broader emission bands situations can be conceived.
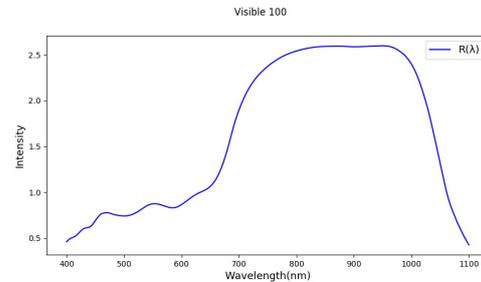

Figure 1: Spectral Response of the PD300-3W with the replaceable filter in. $R(\lambda)$ is the relative sensitivity of the photodiode for the wavelength λ.

The power measured by the photodiode is usually performed on the highest peak of the spectrum and is defined by the following equation, according to the White Paper by the Doctor Efi Rothem "Measuring LED Power and Irradiance with Calibrated Photodiodes" available at Ophir website (Rothem).

$$P_{Meas} = \frac{1}{R[\lambda_0]} \times \int R(\lambda) \times I(\lambda) \, d\lambda \qquad (1)$$

In which P_{Meas} is the power read from the photodiode output display, $R(\lambda)$ is the relative sensitivity of the photodiode for radiation of wavelength λ, $I(\lambda)$ is the spectral intensity of the radiation being measured and λ_0 is the wavelength selected on the photodiode.

Photododiodes are considered valuable and accurate tools when the light source to be studied presents an extremely narrow wavelength such as lasers (Ready, 1971).

To validate Equation 1 it is possible to test if for an ideal single-wavelength light source, accordingly to the manufacturers the optimal situation for use of photodiodes, the power measured by the photodiode is equal to the real power.

The Equation 1 for the ideal light source presented in Figure 2 (example of the spectrum of a laser emitting at 550 nm) becomes:

$$P_{Meas} = \frac{1}{R[555]} \times \int R(\lambda) \times I(\lambda) \, d\lambda \qquad (2)$$

And the real power for any type of light source is given by the Equation 3.

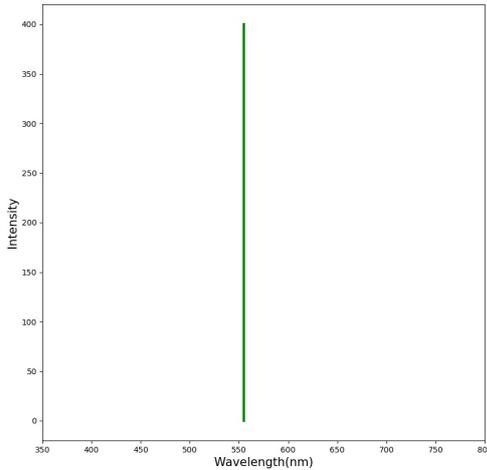$$P_{Real} = \int I(\lambda) \, d\lambda \qquad (3)$$

Figure 2: Spectral distribution of an ideal single wavelength light source.

By the spectrum is easily deductible that $I(\lambda) = 0$ for every wavelength except when $\lambda = 555nm$. So as shown in Equation 4 it is possible to prove that $P_{Meas} = P_{Real}$. For validation of the equality, the value of $\int I(\lambda)$ is not replaced by the intensity value from the spectrum (Figure 2).

$$P_{Meas} = \frac{1}{R[555]} \times \int R[555] \times I(\lambda) \, d\lambda$$

$$P_{Meas} = \frac{\cancel{R[555]}}{\cancel{R[555]}} \times \int I(\lambda) \, d\lambda \qquad (4)$$

$$P_{Meas} = \int I(\lambda) \, d\lambda = P_{Real}$$

This way, it is shown that the Equation 1 for the power measured by the photodiode, is congruent with the fact that photodiodes are accurate direct power meters for narrow band sources.

2 POWER MEASUREMENT

In this section, light hazard measurements will be presented for a smartphone-based handheld fundus camera prototype. This prototype uses two LEDs as light sources, one with a narrow peak on the near infrared (NIR) region of the electromagnetic spectrum and the other emitting broadband white light. The method for examination of the retina with this prototype is characterized by firstly illuminating the fundus with NIR light for guidance. When the examiner is satisfied with the image being observed, a button is pressed and white light is turned on, only for a few milliseconds (typically about 50 to 100 ms is sufficient). The

coloured image obtained is stored and becomes available for consultation on the smartphone. It was established like this, to prevent miosis, an effect that consists on the narrowing of the pupil by action of the Autonomous Nervous System, when visible light reaches the retina (Wang et al., 2016; Tran et al., 2012). As miosis is not verified when infrared light reaches the retina (Shen and Mukai, 2017), to limit the use of white light only to the minimum to obtain a color image of the fundus, this method was chosen to allow a comfortable examination for the patients and to avoid the need of mydriatic agents (drugs that dilate the pupil) (Yuvacı et al., 2015).

The level of the emitted light intensity is controlled by Pulse Width Modulation (PWM) (Dyble et al., 2005). On the smartphone application the operator can select this level on a range between 0 and 100 % of the maximum value allowed.

The emission spectrum of each LED was obtained using a AvaSpec-ULS2048-USB2-VA-50 spectrometer supplied by Avantes. The instrument used to obtain the power values was a photodiode power sensor PD300-3W. Photodiodes principle of operation was already described in Section 1.3.

In order to collect all of the emitted light, in both, spectrum and power measurements, the aperture of the measurement device (spectrometer or photodiode) had to be centered and placed at the focal distance of the optical system covered by the prototype.

Its usable range goes from the near ultraviolet wavelengths to the near infrared region (360-1100 nm) so it was able to recognize the full spectrum of both LEDs.

The White LED is a broadband light source with two peaks, being the first narrow and in the blue region and the other with a wider band and a peak on the yellow\green regions of the spectrum. The NIR LED only has one peak.

The several steps one must consider when performing this type of measurement in such conditions for each LED, may be resumed by the following:

1. Obtain the *spectra* with the spectrometer;

2. Normalize the spectrum according to the maximum counts;

3. Calculate the wavelength of the highest peak by post-processment of the spectrum (in this example python libraries such as NumPy and SciPy were used);

4. In the photodiode select the wavelength obtained in the step 3;

5. Select several levels for the intensity of light through the smartphone application - in this setup

the selected values were 30, 50, 75 and 100 % of the current allowed by the hardware;

6. As photodiodes are very wavelength sensitive, it is needed to multiply the Spectral Response presented in Figure 1 by the Spectrum obtained on step 2;

7. By the direct proportionality relationship between the area beneath the spectral curve and the power, find the real power emitted at each peak wavelength.

The Step 6 is justified by the fact that the Power measured by the Photodiode is given by the Equation 1 in Section 1.3, at the same time that the power emitted by a light source is derived with the Equation 3.

To bring more clarity to the method described before, in the following subsections, not only the final radiant power values obtained will be shown, but also the set of calculations required for each LED.

2.1 White LED

The white LED is a OSLON® Black LUW H9GP supplied by OSRAM. Chromatically it has a temperature of 6500 K, which is considered a cool white with a strong prevalence of lower wavelengths (Violet and Blue regions of the spectrum). As referred previously four different levels for the intensity of the emitted light were measured. The changes on the spectrum along the intensity levels were not representative, only a slight increase on the signal-to-noise ratio with the increase of LED intensity. The normalized spectrometer output for the White LED is presented in Figure 3.

The power measurements obtained on the photodiode are presented in Table 1.
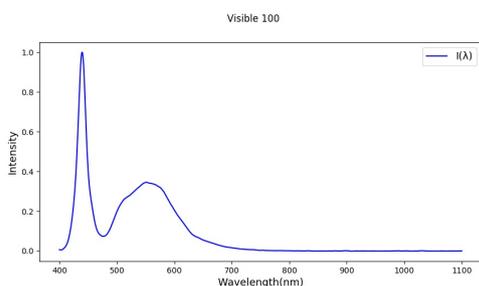

Figure 3: Spectrum of White LED at maximum intensity (100%) obtained with the AvaSoft 2048.

Besides the calculations of these values it was required the multiplication of each spectrum obtained by the spectral response. The curves for the LED spectral intensity, spectral response, and result of its multiplication are presented in Figure 4.
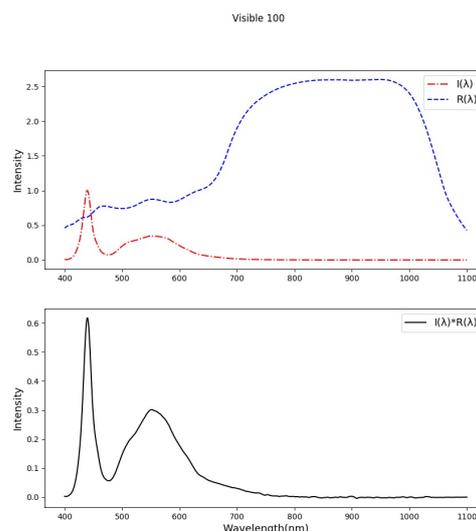

Figure 4: Top - In red is presented $I(\lambda)$, the normalized spectral intensity of the light source and in blue is presented $R(\lambda)$ the relative sensitivity of the photodiode. Bottom - Is presented in black the result of the multiplication of the two curves presented in the Top image - $R(\lambda) \times I(\lambda)$, hereinafter referred as Weighted Spectrum.

To use the Equation 1, the sensitivity of the photodiode at the specific wavelength is needed. For the visible LED, $\lambda_0 = 439$ nm, so $R[\lambda_0] = R[439]$.

The variables needed for the Equation 1:

- $R[439]$ - 0.62

- P_{Meas} - 0.60 mW

Replacing the variables for these values, the Equation 1 becomes:

$$0.60 = \frac{1}{0.62} \times \int R(\lambda) \times I(\lambda) \, d\lambda$$
$$0.372 = \int R(\lambda) \times I(\lambda) \, d\lambda \tag{5}$$

With the last equality of the Equation 5, and considering that the expression $\int R(\lambda) \times I(\lambda) \, d\lambda$ is given by the area beneath the Weighted Spectrum curve, $R(\lambda) \times I(\lambda)$ (Figure 4 - Bottom), a direct proportionality relationship between power and area can be established. The variable Spectrum Area is the area beneath the curve presented in Figure 3, corresponding to the emission spectrum of the LED and named $I(\lambda)$ in Equation 3.

With the variables presented next, the real power (P_{Real}) emitted by the White LED can be calculated.

- Weighted Spectrum Area (WS_{area}) - 49.46

- Spectrum Area (S_{area})- 62.63

- Power with photodiode sensitivity influence (P_{Sens}) - 0.372 mW

Table 1: White LED Measured Power at 439 nm, P_{Meas}, and Real Power, P_{Real}, for each peak and for both peaks.

Wavelength / Smartphone Level	P_{Meas} - 439 nm	P_{Real} - 439 nm	P_{Real} -555 nm	P_{Real} - Total
30	0,18 mW	0,044 mW	0.096 mW	0.140 mW
50	0,31 mW	0,077 mW	0.165 mW	0.242 mW
75	0,45 mW	0,111 mW	0.240 mW	0.351 mW
100	0,60 mW	0,150 mW	0.321 mW	0.471 mW

Considering the relationship of proportionality previously established, the following Equation can be used:

$$P_{Real} = \frac{P_{Sens} \times S_{area}}{WS_{area}}$$
$$P_{Real} = 0.471 \text{ mW} \tag{6}$$

To compare the values obtained with the ISO Norms, it is needed to know the percentage of the total power corresponding to each peak. In order to have an accurate separation of the two peaks a Gaussian Fit function from SciPy library was used. Two Gaussian Fits were considered, one for each peak, with the parameters:

- Wavelength of the Center;
- Amplitude of the Gaussian;
- Width of the Gaussian;

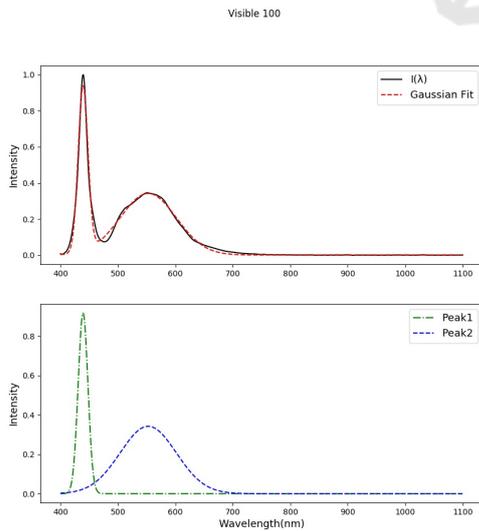The graphical results of the fitting are presented in the Figure 5.

Figure 5: Top - In black is presented I(λ), the spectrum of the light source and in red is presented the Gaussian Fit function. Bottom - Peaks are individually presented, the first in green and the second in blue.

From the area of each peak it is possible to calculate each peak proportion on the total power, as presented by the following equations.

- $A_{Peak1}(\%)$ - 31.8%
- $A_{Peak2}(\%)$ - 68.2%

$$P_{Peak1} = A_{Peak1} \times P_{Real} \quad P_{Peak2} = A_{Peak2} \times P_{Real}$$
$$P_{Peak1} = 0.318 \times 0.471 \quad P_{Peak2} = 0.682 \times 0.471$$
$$P_{Peak1} = 0.150 \text{ mW} \quad P_{Peak2} = 0.321 \text{ mW}$$
$$\tag{7}$$

In Table 1 it is possible to verify the final values for the power of the White LED, for both peak wavelengths.

2.2 NIR LED

The Near Infrared LED is an Infrared Emitter MTE1081C, supplied by Marktech Optoelectronics. The normalized spectrum of the light emitted by the LED is presented in Figure 6. Likewise what occurred with the White LED, the changes on the spectrum along the four intensity levels were not representative. The method is slightly different to the one previously presented for the White LED due to the existence of only one peak.
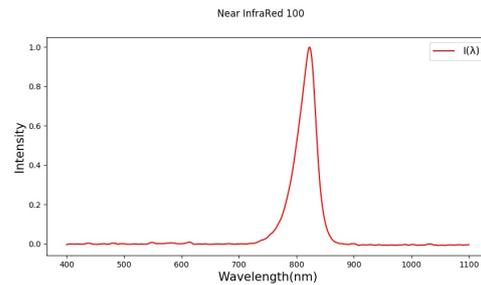

Figure 6: Spectrum of the NIR LED at maximum intensity, (100%) obtained with the AvaSoft 2048.

The power values measured with the Photodiode are presented in Table 2.

The result of the multiplication of the NIR Spectrum by the Spectral Response of the Photodiode is presented in Figure 7.
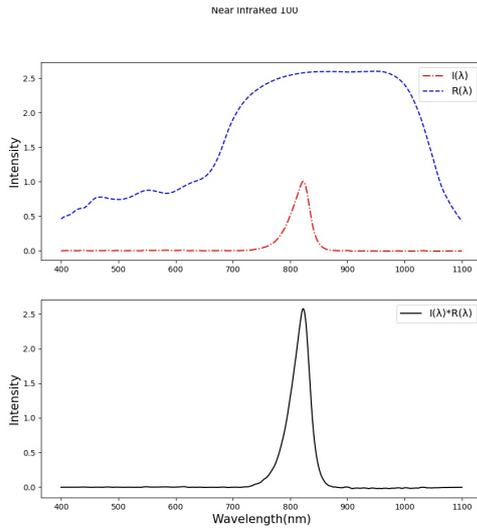
Figure 7: Top - In red is presented I(λ), the spectrum of the light source and in blue is presented R(λ) the relative sensitivity of the photodiode. Bottom - Is presented in black the result of the multiplication of the two curves presented in the top image - R(λ) × I(λ) - Weighted Spectrum.

Similarly to what occurred with the multiplication of the white spectrum by the spectral response (Figure 4), the effect of the wavelength sensitivity of the photodiode is noticeable. The sensitivity of the photodiode for NIR wavelengths is much higher than it is for lower wavelengths, fact that can be confirmed by comparison of the y-scale of the weighted spectral response of both LEDs (Figures 4 and 7 - Bottom).

Calculations will be shown for the maximum intensity level.

- R[820] - 2.57
- P_{Meas} - 0.57 mW

Replacing the above values in Equation 1:

$$0.57 = \frac{1}{2.57} \times \int R(\lambda) \times I(\lambda) \, d\lambda$$
$$1.465 = \int R(\lambda) \times I(\lambda) \, d\lambda \tag{8}$$

The variables needed for the real power (P_{Real}) calculation are:
- Weighted Spectrum Area (WS_{area}) - 106.0
- Spectrum Area (S_{area})- 41.40
- Power with photodiode sensitivity influence (P_{Sens}) - 1.465 mW

$$P_{Real} = \frac{P_{Sens} \times S_{area}}{WS_{area}}$$
$$P_{Real} = 0.57 \text{ mW} \tag{9}$$

The major difference between the used method for each LED is related with the number of peaks. The NIR LED only has one peak and because of that the Gaussian Fit is not required, and P_{Real} can be considered directly proportional to all the area beneath the curve I(λ). With this approximation for the comparison with the ISO norms, all the radiation emitted by the NIR LED is centered at 820 nm.

The results for every level of intensity are presented in Table 2.

Table 2: NIR LED Measured Power at 820 nm - P_{Meas} and NIR LED Real Power at 820 nm - P_{Real}. SL - Smartphone Level; WL- Wavelength.

Power SL	P_{Meas}	P_{Real}
30	0,17 mW	0,168 mW
50	0,30 mW	0,299 mW
75	0,44 mW	0,439 mW
100	0,57 mW	0,570 mW

As can be perceived by comparison of the P_{Meas} and P_{Real} in Table 2, the values are equal or very identical.

This can be explained by the fact that on the region where the NIR LED emits radiation ($\approx$ 758-850 nm - Figure 6), the Photodiode Spectral Response (Figure 1) is considerably flat. Consequently, for the integral $\int R(\lambda) \times I(\lambda) \, d\lambda$, on the spectrum region of interest, R(λ) will be nearly constant and similar to R[820].

3 ISO COEFFICIENTS CALCULATION

In order to ensure the safety of the prototype, the values calculated for the power in the previous section must be converted to quantities that can be compared with the limits displayed on the ISO Norms. So in this section, the calculations required for this conversion will be presented along with the limits applicable to the wavalength of the radiation in question, according to the ISO Standards ISO 15004-2 and ISO 10940 (ISO 15004-2, 2007; ISO 10940, 2009). The first is for light hazard protection of Ophthalmic Instruments and the second deals with the features of Fundus Cameras (including light hazard protection).

As the limits provided on the ISO Norms are presented in irradiance, the areas of the irradiated structures have to be calculated.

The Field of View obtainable with this prototype is 45° so, one way to calculate the retinal area illuminated is by using the formulas on the Equations 10 and 11 (ISO 10940, 2009):

$$\omega = 4\pi\sin^2(\frac{\alpha}{4}) \qquad (10)$$

$$A = (1.7\text{cm})^2 \times \omega \qquad (11)$$

Where ω is the illumination solid angle in steradians, α is the full cone angle in degrees and A is the retinal area illuminated in square centimeters. Considering a Field of View of $45°$ the solid angle is 0.478 sr and consequently the retinal area is 1.381 cm^2.

Knowing the area it is possible to calculate the irradiance with the formula:

$$E = \frac{d\Phi}{dA} \qquad (12)$$

Where E is the irradiance given in mW/cm^2, Φ is the radiant power given in mW, referred as P_{Real} in the previous subsection, and A is the area illuminated in square centimeters. The radiant power was considered to be constant all over the area, so the equation becomes:

$$E = \frac{\Phi}{A} \qquad (13)$$

Therefore, the values for the maximum level of intensity for the peaks of both LEDs are:

- **Retinal Irradiance White - 439 nm Peak =** 0.109 mW/cm^2

- **Retinal Irradiance White - 555 nm Peak =** 0.232 mW/cm^2

- **Retinal Irradiance NIR - 820 nm =** 0.413 mW/cm^2

For the other eye structures the utmost scenario was considered in which the area for calculation of the irradiance was the area of the smallest circle of illumination possible with the prototype. In other words, was considered the area of the circle of illumination at the focal distance from the prototype. It was empirically calculated to be of about 0.071 cm^2, resulting from a circle with 3 mm diameter.

- **Corneal and Anterior Segment Irradiance White - 439 nm Peak** = 2.113 mW/cm^2

- **Corneal and Anterior Segment Irradiance White - 555 nm Peak** = 4.521 mW/cm^2

- **Corneal and Anterior Segment Irradiance NIR - 820 nm** = 8.028 mW/cm^2

As for some hazards the irradiance is weighted according to the wavelength of the radiation, the coefficients for both thermal, $R(\lambda)$, and photochemical aphakic hazard, $A(\lambda)$ provided by the ISO standards, have to be considered for each peak wavelength examined (ISO 15004-2, 2007):

- White LED, 439 nm Peak: $R(\lambda)$ - 1; $A(\lambda)$ - 1;

- White LED, 555 nm Peak: $R(\lambda)$ - 1; $A(\lambda)$ - 0.0078;

- NIR LED, 820 nm Peak: $R(\lambda)$ - 0.58; $A(\lambda)$ - 0;

Considering the principle of operation of the prototype described before, ISO norms compliance was addressed for 4 different situations.

- Continuous NIR LED at maximum intensity;

- Continuous White LED at maximum intensity;

- Pulsed White LED at maximum intensity;

- Real acquisition simulation with the NIR LED at maximum intensity, and pulsed White LED at maximum intensity.

The distinction between continuous and pulsed occurs because in the ISO norms it is considered that when an instrument emits a pulse or a set of pulses that last less than 20 seconds the limits that must be calculated are different from continuous wave instruments (ISO 15004-2, 2007). For each configuration different hazards must be calculated and are going to be presented in the next subsections.

3.1 Continuous NIR

For this configuration the values that have to be calculated are:

- **Unweighted Corneal and Lenticular Infrared Radiation Irradiance, E_{IR-CL};**

$$E_{IR-CL} = \sum_{770}^{2500} E_\lambda \times \Delta\lambda \qquad (14)$$

With,

$$E_\lambda = \frac{d\Phi(\lambda)}{dA \times d\lambda} = \frac{\Phi(\lambda)}{A \times \Delta\lambda} \qquad (15)$$

Where E_λ is the spectral irradiance given in mW/(cm^2.nm), Φ is the radiant power of the radiation, given in mW, A is the area illuminated in square centimeters and $\Delta\lambda$ is the wavelength interval on which the irradiance was measured. This approximation will be considered on every hazard and is only possible because the radiant power was considered to be constant all over the area and all the emission wavelengths near the peak, were considered to be the peak itself. Due to this approximation it is mathematically possible to ignore the dependence on the value of $\Delta\lambda$, as can be observed next.

$$E_{\text{IR-CL}} = \sum_{770}^{2500} \frac{\Phi(\lambda)}{A \times \cancel{\Delta\lambda}} \times \cancel{\Delta\lambda}$$

$$E_{\text{IR-CL}} = \sum_{770}^{2500} \frac{\Phi(\lambda)}{A} \qquad (16)$$

$$E_{\text{IR-CL}} = \sum_{770}^{2500} E$$

$$E_{\text{IR-CL}} = 8.028 \text{ mW/cm}^2$$

- **Unweighted Anterior Segment Visible and Infrared Radiation Irradiance, $E_{\text{VIR-AS}}$;**

$$E_{\text{VIR-AS}} = \sum_{380}^{1200} E_\lambda \times \Delta\lambda \qquad (17)$$

There is only one emitted peak in the NIR spectrum, with 820 nm as center wavelength. So, the result for this hazard is equal to **$E_{\text{IR-CL}}$**, therefore **$E_{\text{VIR-AS}}$** = 8.028 mW/cm^2.

- **Weighted Retinal Visible and Infrared Radiation Thermal Irradiance, $E_{\text{VIR-R}}$;**

$$E_{\text{VIR-R}} = \sum_{380}^{1400} E_\lambda \times R(\lambda) \times \Delta\lambda \qquad (18)$$

$$E_{\text{VIR-R}} = \sum_{380}^{1400} E \times R(\lambda)$$

$$E_{\text{VIR-R}} = 0.413 \times 0.58 \qquad (19)$$

$$E_{\text{VIR-R}} = 0.240 \text{ mW/cm}^2$$

3.2 Continuous White

For this configuration the values that have to be calculated are:

- **Weighted Retinal Irradiance for Photochemical Aphakic Light Hazard, $E_{\text{A-R}}$;**

$$E_{\text{A-R}} = \sum_{350}^{700} E_\lambda \times A(\lambda) \times \Delta\lambda \qquad (20)$$

$$E_{\text{A-R}} = \sum_{350}^{700} E \times A(\lambda)$$

$$E_{\text{A-R}} = 0.109 \times 1 + 0.232 \times 0.0078 \qquad (21)$$

$$E_{\text{A-R}} = 0.109 + 0.00181$$

$$E_{\text{A-R}} = 0.111 \text{ mW/cm}^2$$

- **Unweighted Anterior Segment Visible and Infrared Radiation Irradiance, $E_{\text{VIR-AS}}$;** The

method for the calculation of this hazard was already demonstrated for the NIR LED in the previous subsection, so only the result will be shown.

$$E_{\text{VIR-AS}} = \sum_{380}^{1200} E$$

$$E_{\text{VIR-AS}} = 2.113 + 4.521 \qquad (22)$$

$$E_{\text{VIR-AS}} = 6.634 \text{mW/cm}^2$$

- **Weighted Retinal Visible and Infrared Radiation Thermal Irradiance, $E_{\text{VIR-R}}$;** The method for the calculation of this hazard was already demonstrated for the NIR LED in the previous subsection so, only the result will be shown.

$$E_{\text{VIR-R}} = \sum_{380}^{1400} E \times R(\lambda)$$

$$E_{\text{VIR-R}} = 0.109 \times 1 + 0.232 \times 1 \qquad (23)$$

$$E_{\text{VIR-R}} = 0.341 \text{mW/cm}^2$$

3.3 Pulsed White

For the pulsed mode, information on the duration of each pulse is necessary. In the current prototype, the user can select the duration of flash. Was verified empirically that 0.095 seconds produced fairly good results when imaging an eye model so, it will be considered the time of the pulse for comparison with the ISO Norms comparison. The energy of the flash normally used is the maximum intensity possible for the White LED, so irradiance values are the same as those for the continuous white calculations (Section 3.2).

For the Pulsed Intruments Hazards the results to be compared will take into consideration the spectral radiant exposure, H_λ, which can be derived from the Irradiance, E_λ, according to the following equations.

$$H = \int_{\Delta t} E \times dt = E \times \Delta t \qquad (24)$$

And so,
$$H_\lambda = E_\lambda \times \Delta t \qquad (25)$$

Where E_λ is spectral irradiance, H_λ is spectral radiant power and Δt is the duration of the exposure to the radiation also named exposure time. The value of H_λ is given in mJ/(cm^2.nm).

For the same reason that for the continuous sources, $\Delta\lambda$ is not relevant. For this configuration the values that have to be calculated are:

- **Weighted Retinal Visible and Infrared Radiation Radiant Exposure, $H_{\text{VIR-R}}$;**

$$H_{\text{VIR-R}} = \sum_{380}^{1400} (E_\lambda \times \Delta t) \times R(\lambda) \times \Delta\lambda \qquad (26)$$

$$H_{\text{VIR-R}} = \sum_{380}^{1400} \left(\frac{\Phi(\lambda)}{A} \times \Delta t \right) \times R(\lambda)$$

$$H_{\text{VIR-R}} = \sum_{380}^{1400} E \times \Delta t \times R(\lambda)$$

$$H_{\text{VIR-R}} = 0.109 \times 0.095 \times 1 + 0.232 \times 0.095 \times 1$$

$$H_{\text{VIR-R}} = 0.0324 \text{ mJ/cm}^2$$

(27)

- **Unweighted Anterior Segment Visible and Infrared Radiation Radiant Exposure, $H_{\text{VIR-AS}}$;**

$$H_{\text{VIR-AS}} = \sum_{380}^{1400} H_\lambda \times \Delta\lambda \qquad (28)$$

$$H_{\text{VIR-AS}} = \sum_{380}^{1400} \left(\frac{\Phi(\lambda)}{A} \times \Delta t \right)$$

$$H_{\text{VIR-AS}} = \sum_{380}^{1400} E \times \Delta t \qquad (29)$$

$$H_{\text{VIR-AS}} = 2.113 \times 0.095 + 4.521 \times 0.095$$

$$H_{\text{VIR-AS}} = 0.630 \text{ mJ/cm}^2$$

3.4 Real Acquisition Simulation

Lastly, it is necessary to test the prototype under real acquisition conditions in order to predict if it will fulfill all the safety requirements on real use cases. As was previously referred, the prototype uses NIR light when the operator is performing the retinal alignment so a good image of the retina without provoking mydriasis can be obtained and only acquires the image with white light when observes referable optical structures for the disease being diagnosed (optic disk, vessels...). Consequently, a good simulation of an intended use case can be to consider that the examination takes about **5 minutes**, and **5 images** of the retina are acquired. According to the ISO Norms, in case of consecutive use of different light sources, the limit for radiation reaching each surface of the eye is given by (ISO 15004-2, 2007):

$$\frac{(E,H,L)_1}{Limit_1} + \frac{(E,H,L)_2}{Limit_2} + ... + \frac{(E,H,L)_i}{Limit_i} \leq 1 \quad (30)$$

Where E is the irradiance, H is the radiant exposure, L is the radiance and i is the ith source. As the irradiance and the radiance are analogous, measurements on only one of them are required. In the work here presented only irradiance was used.

For pulsed sources the results obtained must be multiplied by the number of pulses considered so,

when five pulses are considered the spectral exposure results become:

$$H_{5 \text{ Pulses}} = 5 * H_{\text{Single Pulse}} \qquad (31)$$

As a consequence :

- Result $H_{\text{VIR-R}}$ - 0.162 mJ/cm^2
- Result $H_{\text{VIR-AS}}$ - 3.15 mJ/cm^2

The ratio presented above must be verified for different groups of hazards accordingly to the structure they refer to, so the following equations have to be verified.

- Retinal Hazards:

$$\frac{\text{Result } E_{\text{VIR-R}}}{\text{Limit } E_{\text{VIR-R}}} + \frac{\text{Result } H_{\text{VIR-R}}}{\text{Limit } H_{\text{VIR-R}}} =$$
$$= \frac{0.240}{\text{Limit } E_{\text{VIR-R}}} + \frac{0.162}{\text{Limit } H_{\text{VIR-R}}} \qquad (32)$$

- Anterior Segment Hazards:

$$\frac{\text{Result } E_{\text{VIR-AS}}}{\text{Limit } E_{\text{VIR-AS}}} + \frac{\text{Result } H_{\text{VIR-AS}}}{\text{Limit } H_{\text{VIR-AS}}} =$$
$$= \frac{8.028}{\text{Limit } E_{\text{VIR-AS}}} + \frac{3.15}{\text{Limit } H_{\text{VIR-AS}}} \qquad (33)$$

- Corneal and Lenticular Hazards:
  Corneal and Lenticular Hazards only consider radiation emitted between 770 and 2500 nm, so the pulsed white light does not present an hazard for these structures.

As for all the other configurations, the results will be presented in the following section (Section 4).

4 RESULTS AND DISCUSSION

In this Section the comparison of the results obtained for the prototype with the norms currently considered for Ophthalmic Devices will be demonstrated. Hazards results and limits for the modes of operation of the prototype are presented in Table 3. The comparison between the results of the measurements with the limits was performed for the maximum intensity (100%), even though lower levels of light can also allow the acquisition of fairly good images.

Besides the certification that all the results are below Group 1 limits it is necessary to perform the calculations for the real acquisition conditions in order to predict if the prototype will fulfill all the safety requirements on real use cases. As previously stated in subsection 3.4, in case of consecutive use of different light sources, the following equations have to be verified (ISO 15004-2, 2007):

Table 3: Group 1 ISO Norms Compliance. The cells filled in green represent the Hazards for which the results calculated were below the Group 1 Limit.

Mode	Hazard	Result	Group 1 Limit	Compliance
Continuous NIR	E_{IR-CL}	8.028 mW/cm^2	20 mW/cm^2	
	E_{VIR-AS}	8.028 mW/cm^2	4000 mW/cm^2	
	E_{VIR-R}	0.240 mW/cm^2	700 mW/cm^2	
Continuous White	E_{A-R}	0.111 mW/cm^2	0.220 mW/cm^2	
	E_{VIR-AS}	6.634 mW/cm^2	4000 mW/cm^2	
	E_{VIR-R}	0.341 mW/cm^2	700 mW/cm^2	
Single Pulse White	H_{VIR-R}	0.0324 mJ/cm^2	$6t^{\frac{3}{4}}$ = 1.026 J/cm^2 = 1026 mJ/cm^2	
	H_{VIR-AS}	0.630 mJ/cm^2	$25t^{\frac{1}{4}}$ = 13.879 J/cm^2 = 13879 J/cm^2	

- Retinal Hazards:

$$\frac{0.240}{\text{Limit E}_{VIR-R}} + \frac{0.162}{\text{Limit H}_{VIR-R}} =$$
$$= \frac{0.240}{700} + \frac{0.162}{3432} = \qquad (34)$$
$$= 0,000390 \leq 1$$

- Anterior Segment Hazards:

$$\frac{8.028}{\text{Limit E}_{VIR-AS}} + \frac{3.15}{\text{Limit H}_{VIR-AS}} =$$
$$= \frac{8.028}{4000} + \frac{3.15}{20754} = \qquad (35)$$
$$= 0.00216 \leq 1$$

- Corneal and Lenticular Hazards:

For Corneal and Lenticular Hazards there is no Pulsed ratio because on the acquisition mode the prototype only emits white light.

The values for the radiant exposure limits were obtained by replacing the value of t on the equations that set the limits (H_{VIR-R} - $6t^{\frac{3}{4}}$; H_{VIR-AS} - $25t^{\frac{1}{4}}$) by the product of the exposure time for a single pulse and the number of pulses.

5 CONCLUSION

Considering the results presented on the previous section, it is possible to conclude that the EyeFundusScope prototype surpassed the Group 1 Ophthalmic

Device tests, according to the ISO 15004-2 Norm. Group 1 Instruments can be defined as instruments for which no potential light hazard exists (ISO 15004-2, 2007).

If the use case presented in Subsection 3.4 that considers obtaining 5 images during 5 minutes, is not applicable, and a different amount of flashes are directed to the human eye, the calculations required to attest the hazard can be easily performed, by replicating the ones presented in this paper. Considering the differences of orders of magnitude between the result and the limit (presented in the Results subsection 4), it is not likely that a different setup would led to a change of classification of the prototype.

By presenting a method for the measurement of radiant power that uses devices considerably cost-effective when compared to the regularly used equipment (Spectroradiometers (Calandra et al., 2017; Hong et al., 2017)), we believe that the work here presented may be beneficial for all the researchers that want to perform similar tests.

To the best of the authors knowledge, in the literature there is not much information on power measurements for broadband LEDs with photodiodes. Considering this, the work presented in this paper can be of considerable importance in the field of Biomedical Metrology and provide valuable knowledge for the designers of biological and biomedical instruments, who regularly deal with radiation safety issues.

ACKNOWLEDGEMENTS

REFERENCES

Calandra, D. M., Di Martino, S., Riccio, D., and Visconti, A. (2017). Smartphone based pupillometry: An empirical evaluation of accuracy and safety. In Battiato, S., Gallo, G., Schettini, R., and Stanco, F., editors, *Image Analysis and Processing - ICIAP 2017*, pages 433–443, Cham. Springer International Publishing.

Capitán-Vallvey, L. F. and Palma, A. J. (2011). Recent developments in handheld and portable optosensing—a review. *Analytica Chimica Acta*, 696(1):27 – 46.

Chen, H. (2005). Method for manufacturing a triple wavelengths white led.

DeHoog, E. and Schwiegerling, J. (2009). Fundus camera systems: a comparative analysis. *Appl Opt*, 48(2):221–228. 19137032[pmid].

Desmet, K. D., Paz, D. A., Corry, J. J., Eells, J. T., Wong-Riley, M. T., Henry, M. M., Buchmann, E. V., Connelly, M. P., Dovi, J. V., Liang, H. L., Henshel, D. S., Yeager, R. L., Millsap, D. S., Lim, J., Gould, L. J., Das, R., Jett, M., Hodgson, B. D., Margolis, D., and Whelan, H. T. (2006). Clinical and experimental applications of nir-led photobiomodulation. *Photomedicine and Laser Surgery*, 24(2):121–128. PMID: 16706690.

Dyble, M., Narendran, N., Bierman, A., Klein, T., Dyble, M., Narendran, N., Bierman, A., and Klein, T. (2005). Impact of Dimming White LEDs : Chromaticity Shifts Due to Different Dimming Methods.

Eells, J. T., Wong-Riley, M. T., VerHoeve, J., Henry, M., Buchman, E. V., Kane, M. P., Gould, L. J., Das, R., Jett, M., Hodgson, B. D., Margolis, D., and Whelan, H. T. (2004). Mitochondrial signal transduction in accelerated wound and retinal healing by near-infrared light therapy. *Mitochondrion*, 4(5):559 – 567. Mitochondrial Medicine - Developing the Scientific Basis to Medical Management of Mitochondrial Disease.

Feder, R. S., Olsen, T. W., Prum, B. E. J., Summers, C. G., Olson, R. J., Williams, R. D., and Musch, D. C. (2016). Comprehensive adult medical eye evaluation preferred practice pattern guidelines. *Ophthalmology*, 123(1):P209–P236.

Hammer, M. and Schweitzer, D. (2002). Quantitative reflection spectroscopy at the human ocular fundus. *Physics in Medicine & Biology*, 47(2):179.

Hong, S. C., Wynn-Williams, G., and Wilson, G. (2017). Safety of iphone retinal photography. *Journal of Medical Engineering & Technology*, 41(3):165–169. PMID: 27924670.

ISO 10940 (2009). Ophthalmic instruments - Fundus cameras. Standard, International Organization for Standardization, Geneva, CH.

ISO 15004-2 (2007). Ophthalmic instruments - Fundamental requirements and test methods.Part 2: Light Hazard Protection. Standard, International Organization for Standardization, Geneva, CH.

Kelbsch, C., Maeda, F., Strasser, T., Blumenstock, G., Wilhelm, B., Wilhelm, H., and Peters, T. (2016). Pupillary responses driven by iprgcs and classical photoreceptors are impaired in glaucoma. *Graefe's Archive for Clinical and Experimental Ophthalmology*, 254(7):1361–1370.

Malinen, J., Känsäkoski, M., Rikola, R., and Eddison, C. G. (1998). Led-based nir spectrometer module for handheld and process analyser applications. *Sensors and Actuators B: Chemical*, 51(1):220 – 226.

Patrick, D. and Fardo, S. (2000). Industrial electronics: Devices and systems.

Preece, S. J. and Claridge, E. (2002). Monte carlo modelling of the spectral reflectance of the human eye. *Physics in Medicine & Biology*, 47(16):2863.

Rahman, M. Q., Rotchford, A. P., and Ramaesh, K. (2013). Catatrac: a novel red light-emitting diode device for screening cataracts in the developing world. *Eye (Lond)*, 27(1):37–41. 23099916[pmid].

Ready, J. F. (1971). Chapter 2 - measurement techniques. In Ready, J. F., editor, *Effects of High-Power Laser Radiation*, pages 33 – 65. Academic Press.

Rothem, E. Measuring led power and irradiance with calibrated photodiodes. Technical report, Ophir.

Rukmini, A. V., Milea, D., Baskaran, M., How, A. C., Perera, S. A., Aung, T., and Gooley, J. J. (2015). Pupillary responses to high-irradiance blue light correlate with glaucoma severity. *Ophthalmology*, 122(9):1777 – 1785.

Saltmarche, A. E., Naeser, M. A., Ho, K. F., Hamblin, M. R., and Lim, L. (2017). Significant improvement in cognition in mild to moderately severe dementia cases treated with transcranial plus intranasal photobiomodulation: Case series report. *Photomed Laser Surg*, 35(8):432–441. 28186867[pmid].

Schubert, E. (2018). *Light-Emitting Diodes (3rd Edition)*.

Senior, J. (1986). *Optical Fiber Communications: Principles and Practice*. Prentice Hall International (UK) Ltd., Hertfordshire, UK, UK.

Shen, B. Y. and Mukai, S. (2017). A portable, inexpensive, nonmydriatic fundus camera based on the raspberry pi® computer. *Journal of Ophthalmology*, 2017(3):5.

Tran, K., Mendel, T. A., Holbrook, K. L., and Yates, P. A. (2012). Construction of an Inexpensive , Hand-Held Fundus Camera through Modification of a Consumer " Point-and- Shoot " Camera. 53(12):7600–7607.

Wang, Y., Zekveld, A. A., Naylor, G., Ohlenforst, B., Jansma, E. P., Lorens, A., Lunner, T., and Kramer, S. E. (2016). Parasympathetic nervous system dysfunction, as identified by pupil light reflex, and its possible connection to hearing impairment. *PLOS ONE*, 11(4):1–26.

Yuvacı, s., Pangal, E., Yuvacı, S., Bayram, N., Ataş, M., Başkan, B., Demircan, S., and Akal, A. (2015). An evaluation of effects of different mydriatics on choroidal thickness by examining anterior chamber parameters: The scheimpflug imaging and enhanced depth imaging-oct study. *Journal of Ophthalmology*, 2015:1 – 6.